



Cite this: *Dalton Trans.*, 2025, **54**, 5659

Received 3rd February 2025,
Accepted 4th March 2025

DOI: 10.1039/d5dt00271k

rsc.li/dalton

In the field of metal-organic frameworks, the use of yttrium(III) cations and the formation of 3D inorganic building units are rather rare. Here we report an yttrium(III) metal-organic framework based on the V-shaped ditopic linker 4,4'-oxydibenzzoate, oba^{2-} : $[\text{Y}_{16}(\mu\text{-OH}_2)(\mu_3\text{-OH})_8(\text{oba})_{20}(\text{dmf})_4] \cdot 7\text{H}_2\text{O} \cdot 7\text{dmf}$, **1**, which was solvothermally prepared, with single crystal X-ray diffraction revealing an unusual 3D metal secondary building unit. When activated at 200 °C, **1** desolvated to form compound **2**, $[\text{Y}_{16}(\mu\text{-OH}_2)(\mu_3\text{-OH})_8(\text{oba})_{20}] \cdot 6\text{H}_2\text{O}$, retaining the same structure with a 3% shrinkage in unit cell volume.

While research into metal-organic frameworks, popularly known as MOFs,¹ is increasingly engineering related,^{2–5} with devices already on the market⁶ the scientific rationale for synthesising new MOF materials is shifting. The quest for record-breaking surface area, porosity and selectivity is supplemented by a what-if approach using unusual linkers, and in the process, we will acquire new knowledge enabling record-breaking surface areas, porosities and selectivities.

One such what-if scenario involves changing the divergent ditopic linkers, which fit well into the blueprint of existing network topologies due to the perfect mapping of their propagation vectors of 180° onto high symmetry nets, for V-shaped linkers.^{7–20} One such linker is 4,4'-oxydibenzzoic acid (H_2oba)

(Fig. 1) showing an average angle of 125° between the carboxylate carbons and the bridging oxygen (measured on 520 structures in the Cambridge Structural Database²¹).

The other fundamental component of a MOF is the metal secondary building unit, metal-SBU. This part is harder to control and may depend on exact synthesis conditions as well as the linker used.²² It can be as small as a single metal ion, be composed of multinuclear entities of varying geometries, or form infinite 1D units or 2D units. For simplicity, we can refer to the resulting MOFs as dot-, rod-, and sheet-MOFs.²³

This is not simply semantics, as the dimensionality of the metal-SBUs has been implicated in the stability of a MOF,^{24–26} with sheet-MOFs suggested to be more stable than rod-MOFs.

While rod-MOFs are relatively common,²⁷ sheet-MOFs are less so, and their 3D analogues, frame-MOFs (also called MOFs with three-dimensional inorganic connectivity²⁸), are rare. Two examples are ZJNU-120, $\text{Me}_2\text{NH}_2[\text{Sm}_3(5,5'-(5\text{-carboxy}-1,3-phenylene)dicinicotinate)]_3(\text{OH})] \cdot 6\text{dma}$ ²⁸ (dma = *N,N*-dimethylacetamide), featuring a metal-SBU that can be described as a three-periodic (three-dimensional) **srs**-net, and $[\text{Pb}(2,5\text{-dichloroterephthalate})]$ with a metal SBU described by the **peuh** net.²⁹ We here explore the unusual structure and synthesis of the yttrium(III) MOF $[\text{Y}_{16}(\mu\text{-OH}_2)(\mu_3\text{-OH})_8(\text{oba})_{20}(\text{dmf})_4] \cdot 7\text{H}_2\text{O} \cdot 7\text{dmf}$, **1** (Fig. 1), and its desolvated variety **2**.

^aInstitute of Inorganic Chemistry, Christian-Albrechts-University Kiel, Max-Eyth-Straße 2, 24118 Kiel, Germany

^bInorganic Chemistry Department, University of Yaoundé 1, P.O. Box 812, Yaoundé, Cameroon

^cDepartment of Materials and Environmental Chemistry, Stockholm University, 10691 Stockholm, Sweden

^dDipartimento di Chimica, Università degli studi di Milano, Via Golgi 19, 20133 Milano, Italy

^eChemistry and Biochemistry, Dept. of Chemistry and Chemical Engineering, Chalmers University of Technology, SE-41296 Gothenburg, Sweden.

E-mail: ohrstrom@chalmers.se

† Dedicated to Professor Omar M. Yaghi on the occasion of his 60th birthday.

‡ Electronic supplementary information (ESI) available: Crystallographic information files, details of synthesis, characterisation, and topology analysis. CCDC 2240527. For ESI and crystallographic data in CIF or other electronic format see DOI: <https://doi.org/10.1039/d5dt00271k>

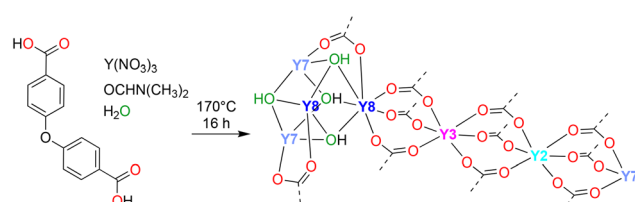


Fig. 1 The linker 4,4'-oxydibenzzoate, oba^{2-} , and its connection to a MOF in $[\text{Y}_{16}(\mu\text{-OH}_2)(\mu_3\text{-OH})_8(\text{oba})_{20}(\text{dmf})_4] \cdot 7\text{H}_2\text{O} \cdot 7\text{dmf}$, **1**. These simple building blocks result in a structure with eight crystallographic independent yttrium(III) ions (four are schematically shown in different colours) forming two interpenetrated metal-SBUs with ten independent oba^{2-} linkers and a unit cell volume of $31\,634(2)\text{ \AA}^3$.



Solvothermal synthesis in a mixture of dimethylformamide, dmf, and water (4 : 1) at 170 °C for 16 h gave $[Y_{16}(\mu\text{-OH}_2)(\mu_3\text{-OH})_8(\text{oba})_{20}(\text{dmf})_4]\cdot7\text{H}_2\text{O}\cdot7\text{dmf}$, **1**, and subsequent heating at 200 °C overnight resulted in the activated form $[Y_{16}(\mu\text{-OH}_2)(\mu_3\text{-OH})_8(\text{oba})_{20}]\cdot6\text{H}_2\text{O}$, **2**.

Single crystal X-ray diffraction of **1** revealed a large unit cell (space group $I4_1$, $a = b = 28.1762(6)$ Å; $c = 39.8472(8)$ Å; $V = 31\,634(2)$ Å³) with eight crystallographically independent yttrium(III) ions and ten independent oba^{2-} linkers; see Fig. 2.

We also note the unusual space group, $I4_1$, one of the Sohncke space groups that preserve chirality, despite there being no intrinsically chiral component in the building blocks. Such MOFs may find use in enantioselective catalysis and separation, or non-linear optics.

While the unit cell of **1** at 31 634(2) Å³ is not exceptionally large, as MOFs with cell volumes over 400 000 Å³ have been reported,³⁰ it falls into a very small category where relatively short, single linkers create exceptional complexity. A classic example is MIL-101,³¹ where two simple SBUs, the trigonal prism $[\text{Cr}_3\text{O}(\text{RCO}_2)_6(\text{X})_3]$ ($\text{X} = \text{OH}^-$ or H_2O) with a diameter of 9 Å and the terephthalate ditopic linker with length around 7.0 Å, give a MOF structure with a unit cell volume of 175 000 Å³.

The key to the large unit cell in MIL-101 is the network topology. MIL-101 has four kinds of six-connected nodes (vertices) and seven kinds of links (edges) and can be described by the topology **mtn-e**.³² This net, in turn, is probably the consequence of the metal-SBU, a flattened trigonal prism.

Also, in **1** the metal-SBU is the key. The central feature is a tetrahedral $[Y_4(\mu_3\text{-OH})_4]$ coordination entity. This entity is also found as a defining part of the dot-MOF $[Y_7(\text{dcpb})_4(\mu_3\text{-OH})_8(\text{HCOO})\cdot(\text{dmf})_5(\text{H}_2\text{O})]\cdot\text{dmf}\cdot\text{H}_2\text{O}$ ($\text{H}_3\text{dcpb} = 3,5\text{-di}(4'\text{-carboxyphenyl})\text{benzoic acid}$), **Y-MOF1**, as a part of a hepta-nuclear metal-SBU;³³ in the rod-MOFs $[Y_6(\text{OH})_8(2,5\text{-pyridinedicarboxylate})_5(\text{H}_2\text{O})_2]$;³⁴ and $[\text{Ln}_5(\mu_2\text{-O})(\mu_3\text{-OH})_5(\text{tca})_2(\text{NO}_3)_2(\text{CH}_3\text{COO})(\text{H}_2\text{O})_2]\cdot\text{NH}(\text{CH}_3)_2\cdot\text{dma}\cdot(\text{H}_2\text{O})_3$, ($\text{H}_3\text{tca} = 4,4',4''\text{-tricarboxy-triphenylamine}$);³⁵ and finally in the sheet-MOF $[Y_5(\text{OH})_6(\text{HCOO})_3(\text{CO}_3)_2(\text{C}_4\text{O}_4)]\cdot2.5\text{H}_2\text{O}$.³⁶

In **1**, however, each $[Y_4(\mu_3\text{-OH})_4]^{8+}$ entity connects in all four directions of the tetrahedron to a short $[Y_2(\text{RCOO})_9]$ chain con-

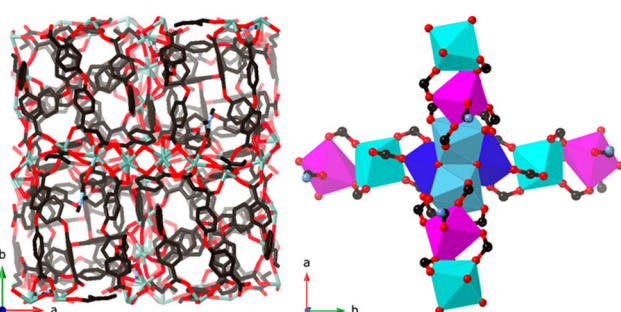


Fig. 2 X-ray single crystal structure of $[Y_{16}(\mu\text{-OH}_2)(\mu_3\text{-OH})_8(\text{oba})_{20}(\text{dmf})_4]\cdot7\text{H}_2\text{O}\cdot7\text{dmf}$, **1**. Left: unit cell ($I4_1$, $a = b = 28.1762(6)$ Å; $c = 39.8472(8)$ Å) view in the z -axis direction with hydrogens omitted for clarity. Right: part of one of the two independent dia-nets that form the 3D-metal SBUs with the same colour coding as in Fig. 1.

necting to the next $[Y_4(\mu_3\text{-OH})_4]^{8+}$ entity forming a **dia**-net. This accounts for four of the eight crystallographic yttrium ions. The other four assemble into an identical **dia**-net, related to the first by translation (type I interpenetration³⁷, see Fig. 3, left), giving an overall topology of the metal-SBU as **dia-c**.

These 3D metal-SBUs, with cations joined by carboxylate groups and the $\mu_3\text{-OH}$ of the tetrahedra, are then further bridged by the $\text{oba}^{2-}\text{-C}_6\text{H}_4\text{-O-C}_6\text{H}_4\text{-}$ organic SBU forming a fully connected non-interpenetrated MOF. As can be deduced from Fig. 1 there are nine of these in three triplets protruding from a $[\text{Y}_2(\text{RCOO})_9]$ entity between two $[Y_4(\mu_3\text{-OH})_4]$ tetrahedra, and one symmetrically independent oba^{2-} linker from each tetrahedron, making a total of ten crystallographically independent oba^{2-} bridges. This has been illustrated in Fig. 3, right.

In this way, the framework of **1** can be topologically described using the straight rod (STR) approach by adding mid-points between the metals and connecting the carbon atom of the COO bridge to the midpoint of the rod.^{38,39} The network analysis of the network in **1** is complex, as it involves two 6-connected vertices (the tetrahedral nodes of the two different metal-SBUs are 4-connected in the SBU and then bridges with two oba^{2-} linkers) and six 5-connected vertices (2 connections within the metal-SBUs and 3 via the oba^{2-} linkers), see Fig. 4.

Hardly surprising, this does not reduce to any of the high symmetry common nets, but to a chiral 5⁶·6²·c net, thus an 8-nodal net (see the ESI† for further information).

There are no apparent channels when looking at the structure of **1**, and pore analysis using mercury reveals only 4% solvent-accessible volume, but 19% based on the contact surface (probe radius: 1.2 Å), yet these seem to be isolated pockets rather than channels (see the ESI†).

Indeed, using a solvent mask routine during structure refinement (see the ESI†) we detected three distinct pockets

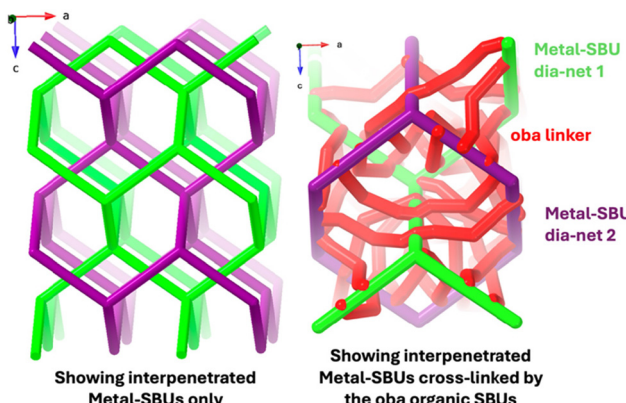


Fig. 3 Left: when we remove the connections through the $\text{-C}_6\text{H}_4\text{OC}_6\text{H}_4\text{-}$ organic part, retaining only the carboxylates, we see that the metal-SBUs in $[Y_{16}(\mu\text{-OH}_2)(\mu_3\text{-OH})_8(\text{oba})_{20}(\text{dmf})_4]\cdot7\text{H}_2\text{O}\cdot7\text{dmf}$, **1**, form two interpenetrated dia-nets each held together by bridging $\text{Y}-\text{C}=\text{O}-\text{Y}$. Right: the bridging of the two metal-SBUs by the $\text{oba}^{2-}\text{-C}_6\text{H}_4\text{-O-C}_6\text{H}_4\text{-}$ organic SBU in red. For clarity some of the oba^{2-} links have been omitted.



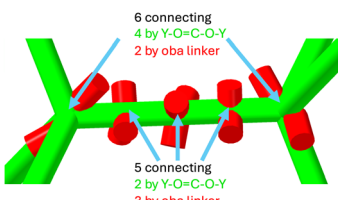


Fig. 4 The network description of $[\text{Y}_{16}(\mu\text{-OH}_2)(\mu_3\text{-OH})_8(\text{oba})_{20}(\text{dmf})_4]\cdot 7\text{H}_2\text{O}\cdot 7\text{dmf}$, **1**, involves two 6-connected vertices (the tetrahedral nodes of the two different metal-SBUs are 4-connected in the SBU and then bridge with two oba^{2-} linkers) and six 5-connected vertices (two connections within the metal-SBUs and 3 via the oba^{2-} linkers).

with volumes and electron densities consistent with a total of 6.5 dmf molecules and 5.5 water molecules per formula unit. Elemental analysis of **1** indicates seven dmf and seven H_2O molecules per formula unit, while thermogravimetric analysis (TGA) results indicate the composition $[\text{Y}_{16}(\mu\text{-OH}_2)(\mu_3\text{-OH})_8(\text{oba})_{20}(\text{dmf})_4]\cdot 7\text{H}_2\text{O}\cdot 7\text{dmf}$.

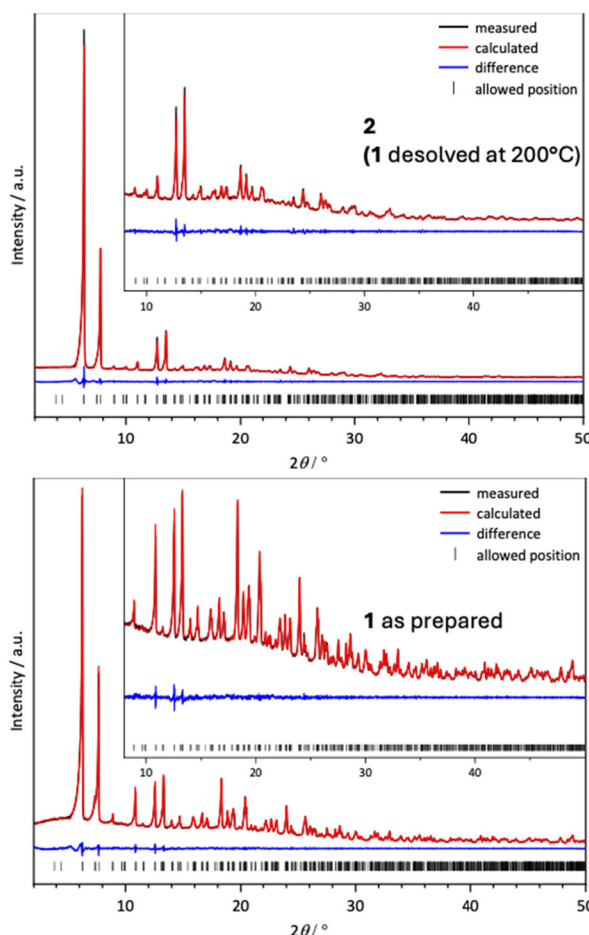


Fig. 5 $[\text{Y}_{16}(\mu\text{-OH}_2)(\mu_3\text{-OH})_8(\text{oba})_{20}(\text{dmf})_4]\cdot 7\text{H}_2\text{O}\cdot 7\text{dmf}$, **1**, can be desolvated at 200 °C to yield **2**, $[\text{Y}_{16}(\mu\text{-OH}_2)(\mu_3\text{-OH})_8(\text{oba})_{20}]\cdot 6\text{H}_2\text{O}$. The top figure shows Pawley fit on the powder data of **2** ($R_{\text{wp}} 2.96\%$) and the bottom figure the fit for **1** ($R_{\text{wp}} 2.19\%$). Both PXRD diffractograms were collected at room temperature.

$\text{OH})_8(\text{oba})_{20}(\text{dmf})_4]\cdot 5\text{H}_2\text{O}\cdot 6\text{dmf}$, data that are consistent given the handling of the sample in air and variations in relative humidity. For the formula of **1**, we use the elemental analysis results.[§]

TGA indicates the possibility of thermal stability up to 400 °C (Fig. S5[‡]) consistent with the idea that higher dimensionality of metal SBUs should be more stable.

Despite the apparent lack of channels, **1** can be desolvated by heating to 200 °C overnight leading to compound **2** that we formulate, based on elemental analysis, as $[\text{Y}_{16}(\mu\text{-OH}_2)(\mu_3\text{-OH})_8(\text{oba})_{20}]\cdot 6\text{H}_2\text{O}$. The X-ray powder pattern of **2** was successfully fitted by a Pawley procedure ($R_{\text{wp}} 2.96\%$) starting from the initial cell parameters and space group of **1**. This resulted in a 3% smaller cell volume. As a control, we also conducted a Pawley fit on the powder data of **1**, yielding similar fitting parameters ($R_{\text{wp}} 2.19\%$); see the ESI[‡] and Fig. 5.

At 298 K **2** shows a modest uptake of CO_2 of 0.85 mmol g⁻¹ at 100 kPa, in reasonable agreement with the void space in the structure if we use van Heerden and Barbour's 50% rule of thumb,⁴² which gives an estimate of 0.61 mmol g⁻¹ uptake of CO_2 (see the ESI[‡]). The PXRD pattern in Fig. S1[‡] shows that **2** remains unchanged after the sorption experiment.

In conclusion, the use of V-shaped rather than divergent high-symmetry linkers can yield complex MOF structures, and potentially facilitate the formation of materials with 3D metal-SBUs, herein described as frame-MOFs. These highly interconnected motifs may yield materials with superior stability and lead to the discovery of previously unobserved network structures. Moreover, this study highlights the rarely found class of frame-MOFs, having metal SBUs periodic in three dimensions, 3D-SBUs. This has implications on our thinking of the whole class of metal-organic frameworks and coordination polymers—how they are constructed and synthesised.

Data availability

The data supporting this article have been included as part of the ESI.[‡]

1 have been deposited at the CCDC under 2240527[‡]. All other data presented in this study are available in the article.

Conflicts of interest

There are no conflicts to declare.

Acknowledgements

L. Ö thanks the Swedish Research Council and D. M. P. thanks the MUR for the grant PRIN2020 "Nature Inspired Crystal Engineering (NICE)" and Prof. Vladislav A. Blatov at the Samara Center for Theoretical Materials Science for providing the free ToposPro software (<https://topospro.com>). C. L. F. D.

thanks DAAD, the Deutscher Akademischer Austauschdienst, for a stipend.

References

[§]The reported MOFs were characterised by single crystal diffraction (1) (CCDC 2240527†) PXRD, TGA, IR, and elemental analysis. Topologies were analysed with ToposPro⁴⁰ and SYSTRE.⁴¹ Gas sorption analysis was run on a MICROTRAC BELSORP MINI X. Pawley fits for the powder patterns were conducted with TOPAS Academic.⁴³

- 1 S. R. Batten, N. R. Champness, X.-M. Chen, J. Garcia-Martinez, S. Kitagawa, L. Öhrström, M. O'Keeffe, M. P. Suh and J. Reedijk, *Pure Appl. Chem.*, 2013, **85**, 1715–1724.
- 2 To date and published in 2024, the top five Web of Science Categories for a search of “Metal-Organic Frameworks” are: Materials Science Multidisciplinary 1669; Chemistry Multidisciplinary 1544; Chemistry Physical 1443; Nanoscience Nanotechnology 920; Engineering Chemical 811.
- 3 T. Jia, Y. F. Gu and F. T. Li, *J. Environ. Chem. Eng.*, 2022, **10**, 108300.
- 4 T. Lassitter, N. Hanikel, D. J. Coyle, M. I. Hossain, B. Lipinski, M. O'Brien, D. B. Hall, J. Hastings, J. Borja, T. O'Neil, S. E. Neumann, D. R. Moore, O. M. Yaghi and T. G. Glover, *Chem. Eng. Sci.*, 2024, **285**, 119430.
- 5 X. G. Liu, Y. Y. Shan, S. T. Zhang, Q. Q. Kong and H. Pang, *Green Energy Environ.*, 2023, **8**, 698–721.
- 6 Z. Chen, M. C. Wasson, R. J. Drout, L. Robison, K. B. Idrees, J. G. Knapp, F. A. Son, X. Zhang, W. Hierse, C. Kühn, S. Marx, B. Hernandez and O. K. Farha, *Faraday Discuss.*, 2021, **225**, 9–69.
- 7 S. F. Du, X. Y. Yu, G. L. Liu, M. Zhou, E. S. M. El-Sayed, Z. F. Ju, K. Z. Su and D. Q. Yuan, *Cryst. Growth Des.*, 2021, **21**, 692–697.
- 8 C. M. Ngue, Y. H. Liu, M. Leung and K. L. Lu, *Inorg. Chem.*, 2021, **60**, 11458–11465.
- 9 T. Rabe, E. S. Grape, T. A. Engesser, A. K. Inge, J. Ströh, G. Kohlmeyer-Yilmaz, M. Wahiduzzaman, G. Maurin, F. D. Sönnichsen and N. Stock, *Chem. – Eur. J.*, 2021, **27**, 7696–7703.
- 10 T. Rabe, E. S. Grape, H. Rohr, H. Reinsch, S. Wöhlbrandt, A. Lieb, A. K. Inge and N. Stock, *Inorg. Chem.*, 2021, **60**, 8861–8869.
- 11 E. P. Asiwal, D. S. Shelar, C. S. Gujja, S. T. Manjare and S. D. Pawar, *New J. Chem.*, 2022, **46**, 12679–12685.
- 12 J. J. Huang, D. Zhao and G. J. Yin, *Chin. J. Struct. Chem.*, 2022, **41**, 2203030–2203039.
- 13 L. Yu, S. Ullah, K. Zhou, Q. B. Xia, H. Wang, S. Tu, J. J. Huang, H. L. Xia, X. Y. Liu, T. Thonhauser and J. Li, *J. Am. Chem. Soc.*, 2022, **144**, 3766–3770.
- 14 J. Gosch, V. Guiotto, F. Steinke, E. S. Grape, C. Atzori, K. Mertin, T. Otto, N. Ruser, C. Meier, D. M. Venturi, A. K. Inge, K. A. Lomachenko, V. Crocellà and N. Stock, *Inorg. Chem.*, 2023, **62**, 20929–20939.
- 15 J. Gosch, D. M. Venturi, E. S. Grape, C. Atzori, L. Donà, F. Steinke, T. Otto, T. Tjardts, B. Civalleri, K. A. Lomachenko, A. K. Inge, F. Costantino and N. Stock, *Inorg. Chem.*, 2023, **62**, 5176–5185.
- 16 M. B. Kim, A. J. Robinson, M. L. Sushko and P. K. Thallapally, *J. Ind. Eng. Chem.*, 2023, **118**, 181–186.
- 17 W. W. Zhong, F. D. Firuzabadi, Y. Hanifehpour, X. Zeng, Y. J. Feng, K. G. Liu, S. W. Joo, A. Morsali and P. Retailleau, *Inorganics*, 2023, **11**, 11050184.
- 18 M. Xiong, A. Mohanty, D. H. Liao, L. Lu, W. Zhang, J. Wang, M. Muddassir, S. Al-Sulaimi and Y. Pan, *J. Mol. Struct.*, 2024, **1297**, 136958.
- 19 A. M. Plonka, D. Banerjee, W. R. Woerner, Z. J. Zhang, J. Li and J. B. Parise, *Chem. Commun.*, 2013, **49**, 7055–7057.
- 20 D. Banerjee, S. K. Elsaiedi and P. K. Thallapally, *J. Mater. Chem. A*, 2017, **5**, 16611–16615.
- 21 C. R. Groom, I. J. Bruno, M. P. Lightfoot and S. C. Ward, *Acta Crystallogr., Sect. B: Struct. Sci., Cryst. Eng. Mater.*, 2016, **72**, 171–179.
- 22 L. Öhrström and F. M. Amombo Noa, *Metal-Organic Frameworks*, American Chemical Society, 2021.
- 23 F. M. Amombo Noa, M. Abrahamsson, E. Ahlberg, O. Cheung, C. R. Göb, C. J. McKenzie and L. Öhrström, *Chem.*, 2021, **7**, 2491–2512.
- 24 C. Healy, K. M. Patil, B. H. Wilson, L. Hermanspahn, N. C. Harvey-Reid, B. I. Howard, C. Kleinjan, J. Kolien, F. Payet, S. G. Telfer, P. E. Kruger and T. D. Bennett, *Coord. Chem. Rev.*, 2020, **419**, 20.
- 25 N. Hanikel, M. S. Prévot, F. Fathieh, E. A. Kapustin, H. Lyu, H. Wang, N. J. Diercks, T. G. Glover and O. M. Yaghi, *ACS Cent. Sci.*, 2019, **5**, 1699–1706.
- 26 P. Siman, C. A. Trickett, H. Furukawa and O. M. Yaghi, *Chem. Commun.*, 2015, **51**, 17463–17466.
- 27 A. Schoedel, M. Li, D. Li, M. O'Keeffe and O. M. Yaghi, *Chem. Rev.*, 2016, **116**, 12466–12535.
- 28 X. Wang, L. Yue, P. Zhou, L. Fan and Y. He, *Inorg. Chem.*, 2021, **60**, 17249–17257.
- 29 S. Khan, S. Naaz, S. Ahmad, R. M. Gomila, A. Chanthapally, A. Frontera and M. H. Mir, *Chem. Commun.*, 2024, **60**, 10370–10373.
- 30 T. Li, M. T. Kozlowski, E. A. Doud, M. N. Blakely and N. L. Rosi, *J. Am. Chem. Soc.*, 2013, **135**, 11688–11691.
- 31 G. Ferey, C. Mellot-Draznieks, C. Serre, F. Millange, J. Dutour, S. Surble and I. Margiolaki, *Science*, 2005, **309**, 2040–2042.
- 32 M. O'Keeffe and O. M. Yaghi, *Chem. Rev.*, 2012, **112**, 675–702.
- 33 P. Qu, M.-H. Zhang and J.-W. Zhang, *Inorg. Chem. Commun.*, 2023, **151**, 110623.
- 34 M. S. M. Abdelbaky, Z. Amghouz, E. Fernández-Zapico, S. García-Granda and J. R. García, *J. Solid State Chem.*, 2015, **229**, 197–207.
- 35 H. Wu, S. Zhang, M. Li, C. Qiao, L. Sun, Q. Wei, G. Xie, S. Chen and S. Gao, *ChemistrySelect*, 2016, **1**, 3335–3342.
- 36 Y.-T. Huang, Y.-C. Lai and S.-L. Wang, *Chem. – Eur. J.*, 2012, **18**, 8614–8616.



37 V. A. Blatov, L. Carlucci, G. Ciani and D. M. Proserpio, *CrystEngComm*, 2004, **6**, 377–395.

38 L. S. Xie, E. V. Alexandrov, G. Skorupskii, D. M. Proserpio and M. Dincă, *Chem. Sci.*, 2019, **10**, 8558–8565.

39 P. Tshuma, B. C. E. Makhubela, L. Öhrström, S. A. Bourne, N. Chatterjee, I. N. Beas, J. Darkwa and G. Mehlana, *RSC Adv.*, 2020, **10**, 3593–3605.

40 V. A. Blatov, A. P. Shevchenko and D. M. Proserpio, *Cryst. Growth Des.*, 2014, **14**, 3576–3586.

41 O. Delgado-Friedrichs and M. O'Keeffe, *Acta Crystallogr., Sect. A: Found. Crystallogr.*, 2003, **59**, 351–360.

42 D. P. van Heerden and L. J. Barbour, *Chem. Soc. Rev.*, 2021, **50**, 735–749.

43 A. A. Coelho, TOPAS and, TOPAS-Academic: an optimization program integrating computer algebra and crystallographic objects written in C++, *J. Appl. Crystallogr.*, 2018, **51**, 210–218, DOI: [10.1107/S1600576718000183](https://doi.org/10.1107/S1600576718000183).